

General Disclaimer

One or more of the Following Statements may affect this Document

- This document has been reproduced from the best copy furnished by the organizational source. It is being released in the interest of making available as much information as possible.
- This document may contain data, which exceeds the sheet parameters. It was furnished in this condition by the organizational source and is the best copy available.
- This document may contain tone-on-tone or color graphs, charts and/or pictures, which have been reproduced in black and white.
- This document is paginated as submitted by the original source.
- Portions of this document are not fully legible due to the historical nature of some of the material. However, it is the best reproduction available from the original submission.

DESIGN CONSIDERATIONS IN MECHANICAL FACE SEALS FOR IMPROVED PERFORMANCE

II. LUBRICATION

by

Lawrence P. Ludwig
National Aeronautics and Space Administration
Lewis Research Center
Cleveland, Ohio 44135

and

Harold F. Greiner
Sealol, Inc.
Providence, Rhode Island

ABSTRACT

The importance of sealing technology in our industrial, chemical-orientated society in regard to maintenance and environmental contamination is pointed out. It is stated that seal performance (leakage, life) is directly related to seal lubrication, which is a mechanism which is not well understood. Current thinking in regard to seal lubrication is reviewed; the effect of energy dissipation in the thin lubricating film separating the sealing faces is pointed out, and the results of vaporization due to heating are illustrated. Also, hydrodynamic lubrication is reviewed, and an inherent tendency for the seal to operate with angular misalignment is pointed out. Recent work on hydrostatic effects is summarized and the conditions for seal instability are discussed. Four different modes of seal lubrication are postulated with the mode type being a strong function of speed and pressure.

INTRODUCTION

The long operating life of some seals for liquids suggests that the primary-seal faces (which are in relative rotational motion) are separated by a lubricating film; the lubricating film being established either by hydrodynamic or hydrostatic forces (in some cases both types of forces may be operable). In some applications, the seals operate in a boundary lubrication regime, the lubricating film being so thin that considerable solid surface sliding contact takes place. Many theories to explain full film lubrication of face seals have been developed and reported (see refs. (1) through (11)); these theories were reviewed in a recent paper (ref. (11)). A basic difficulty is found in the fact that the lubricating film is very thin (in the range of 1 micron or less) and, therefore, very small surface irregularities, elastic displacements (thermal bumps, etc.), and seal face runout motions have a dramatic effect on the lubrication of the seal.

In a companion paper (ref. (12)) it was pointed out maintenance costs due to seal failure can be very high and that leakage through seals is a major concern if the fluid is toxic or is a carcinogenic substance. In this regard, the EPA recently pointed out that our industrial chemical-oriented society introduces about 2000 new chemicals per year with nearly 30,000 different chemicals being in commercial production. Not all these chemicals are toxic, but there is a great risk that some of these chemicals now being produced could later be found to be dangerous to human health. These considerations place an additional burden on the sealing industry to produce seal

systems which perform properly during the entire design life. As indicated previously, there is a need for better understanding of seal lubrication mechanisms, also seal leakage must be better characterized with attention given to very low leakage levels that may be only in the form of vapors. This question of leakage rate is related to the lubrication mechanisms, and therefore, may only be answered after seal lubrication is better understood.

The objective of this work is to review the state-of-the-art of liquid lubricated face seals and to summarize current thinking in regard to seal lubrication. Attention will be restricted to that class of seals which operate on a full lubricating film, that is, boundary lubrication and dry operation will not be addressed.

DISCUSSION

Lubrication, Thermal Effects

Temperature at the primary seal surfaces is a critical controlling factor of seal life and wear rate, and for this reason certain types of applications require seal cooling. Considerable heat can be generated at the primary seal even if the seal is operating under full film lubrication. For example, ref. (13) reports process liquid boiling in the primary seal at relatively low sliding speeds. A glass rotating seal seat was used and this permitted direct observation of the interface. It was found that the gap between the seal faces contained two distinct regions: a continuous liquid-film region next to the sealed liquid, and a region of vapor and liquid from the liquid interface out to the atmospheric edge. This is illustrated in fig. 1. Also, the glass seat permitted infra-red measurements and indicated that boiling temperatures were reached at the liquid interface.

In ref. (14) a thermal analysis of phase change in liquid lubricated face seals is developed. This analysis revealed many important effects which are associated with a phase change, and some of these are:

(1) A phase change within the primary seal produces a pressure profile which is very different from the classical linear profile associated with liquids. Phase change causes a greater opening force; the resulting gradients in pressure and temperature are illustrated in fig. 2, which was taken from ref. (14).

The significance of this phase change is illustrated in fig. 3 where classical pressure gradients across the primary seal are compared. Note that when the primary sealing gap is filled with liquid the pressure gradient is linear (for parallel surfaces). For gas or vapor the pressure gradient is parabolic and the load capacity (or opening force) is greater

E-9298-2

than that for the liquid. The important point is that the largest opening force is produced when a liquid to vapor interface is formed within the seal gap.

(2) Leakage decreases when the phase change occurs.

(3) For a given configuration there are two film thicknesses which will support the same load but only the larger thickness is stable (see fig. 4). Also for a given seal configuration, there are two angular velocities which produce the same load, only the upper one being stable; finally, there are two bulk temperatures which produce the same load, but the seal is stable only at the upper bulk temperature.

(4) The conductivity of the seal rings has a significant effect on the location of the liquid to vapor interface; increasing the thermal conductivity shifts the liquid to vapor interface towards the exit.

(5) The seal load is a function of a parameter h/ω^2 and this is illustrated in fig. 5 from ref. (14). In fig. 5, note that the maximum seal load occurs when the liquid to vapor interface is located at a radius of 5.599×10^{-2} meters. To the right of the maximum load point the seal is stable because any decrease in film thickness increases the seal load support capability, that is, the film has positive film stiffness; to the left of the maximum load capacity the film stiffness is negative and the seal unstable.

Identification of the parameter, h/ω^2 , as having significance comes from consideration of the power loss due to fluid film shear.

$$P = \tau Ar \omega$$

where

P = power loss

τ = μ dv/dh (Newton law of viscous shear)

in which

μ = fluid viscosity

dv/dh = velocity gradient in the fluid film

A = area wetted by fluid

r = radius

ω = angular velocity

Since $dv = r\omega$ and $dh =$ gap height, h

$$P = \underbrace{\mu}_{\text{fluid property}} \underbrace{Ar^2}_{\text{geometric parameter}} \underbrace{\omega^2/h}_{\text{operating parameter}}$$

The thermal analysis of ref. (14) reveals that for a given configuration and face loading, two operating film thicknesses exist, one stable and one unstable; this suggests that hydrodynamic and hydrostatic must, at times, work in conjunction with the thermal two phase effects in order to maintain seal stability.

Lubrication, Hydrodynamic Effects

There is considerable reported evidence that in a large class of radial face seals, hydrodynamic lubrication is responsible for maintaining separation of the seal faces. Many theories to explain this seal lubrication have been developed and reported (angular misalignment, surface waviness, etc.). These theories, which are based on the inclined-slider-bearing principle, can be divided into two general groups: the

inclined-slider macrogeometry and the inclined-slider microgeometry. These published theories which have given very valuable insight as to the nature of seal lubrication are summarized in tables I and II (from ref. (11)).

Thermal effects can cause waviness (see fig. 6 from companion paper, ref. (12)) in the faces of the primary-seal. And this waviness produces hydrodynamic pressures that can act to separate the seal faces, essentially the mechanism is that of an inclined slider bearing.

Reference (4) develops a theory of hydrodynamic load support based on thermal deformation of the metal surface in a seal having a carbon surface mated to a metal surface. The carbon surface is considered to be flat, but the metal surface has a network of scratches several micrometers deep. The distance between scratches is a few tenths of a millimeter. Under the action of a pressure differential the fluid flows with greater velocity along the scratches than in the remaining portions. The surfaces are assumed to be separated by a fluid film. Relative motion causes uneven heating of the fluid film and metal wall, the temperature being lowest at the scratches, where the leakage velocity is highest and film thickness is greatest. Moving away from a scratch in the direction of motion, the fluid progressively heats up and the wall expands unevenly. Therefore, the portion of the metal face between scratches takes on a small slope, and a multiplicity of small converging wall geometries are thus formed. Thus, hydrodynamic forces are generated.

In refs. (15) and (16) the importance of maintaining a fluid lubricating film is stressed. For very high pressure (to 2413 N/cm^2 (3000 psi)), ref. (15) reveals that radial slots cause thermally induced wedge deformation that promotes hydrodynamic effects. This is referred to as a hydrodynamic type of seal. One hydrodynamic seal described in ref. (16) is shown in fig. 7. The construction of this hydrodynamic seal is similar to that of a conventional face seal except that the primary-ring face contains circular grooves (fig. 7). Seal rotation causes the sealed liquid to circulate through these grooves, and thus the grooved region is cooler than the other regions. Therefore, thermal deformations produce wedge geometries (inclined slider bearing) that give rise to hydrodynamic forces. Figure 7 also illustrates the hydrodynamic force (pressure profile) that is built up in the region of the circular grooves. This type of seal apparently maintains a more efficient hydrodynamic action (than a conventional face seal) as pressure and speed increase. Thus, it has superior performance. Successful operation at pressure to 2413 N/cm^2 (3000 psi) and 101 m/sec (333 ft/sec) for thousands of hours has been reported (refs. (15) and (16)).

Reference (17) has shown that solid surfaces in parallel sliding and separated by a viscous liquid film can be thermally unstable (develop waviness) when a critical velocity is exceeded. This critical velocity is a function of the nominal film thickness, liquid viscosity, thermal conductivity and thermal expansion coefficient. Basically, the sequence of events is visualized to occur as follows:

(1) In the primary seal the film thickness will not be absolutely uniform, variations will occur because of machining tolerances, clamping distortions, etc.

(2) The heat dissipation is higher at the point where the film is thinner and hot spots (waviness) develop.

(3) Below a critical speed this waviness tends to be self-stabilizing because of the associated hydrodynamic forces which act to increase the film thickness.

4. Beyond a critical sliding speed, increases in wave amplitude are unstable and rubbing contact occurs.

Reference (18) reports the development of waviness during operation in the softer material faces of a wide variety of seals. The wave amplitude was generally in the range of 0.25 to 10 microns. And the study revealed that surface waviness of considerable magnitude developed in all seals which experienced gross wear, the wave amplitude increasing with wear.

Reference (19) presents data which rather convincingly show that seals can operate with hydrodynamic lubrication, and ref. (19) attributes this hydrodynamic lubrication to surface waviness. The coefficients of friction measured (as low as 0.02) are typical of hydrodynamic lubrication. And this agrees with the data from ref. (20), in which it was pointed out that, when the coefficient of friction is plotted as a function of the $\eta U/p$ parameter, the curve has the same general shape as those for journal bearings. Thus, the evidence for hydrodynamic lubrication is very strong.

Reference (19) considers two waves in the circumferential direction, and the load generation capacity is based on this two-wave assumption. In effect, the seal is treated analytically as a plain inclined slider bearing and a simplified Reynolds equation (short-bearing approximation) is solved explicitly for the generated pressure.

Pape (ref. (6)) concludes that sealing faces generally operate in a fully hydrodynamic manner. He states that the mechanism causing hydrodynamic lubrication or load support is wedge action and that the minute waviness of the faces, of the order of 0.10 micrometer, which occurs in the circumferential direction can generate a film in the range of 1 micrometer thick. The analysis of ref. (6) is based on the Reynolds equation which is two dimensional and time dependent (see Table I). Surface waviness, which is assumed, is the source of the load capacity. Considerable attention is given to obtaining correct continuity of flow conditions as affected by cavitation regions.

Relative angular misalignment of the primary-seal faces (see fig. 6) produces a converging/diverging film shape in the circumferential direction; thus the primary-seal can act as an inclined slider bearing, when in this configuration. This is essentially a single wave and the hydrodynamics load support produced by this configuration has been analyzed by ref. (1) (see table II). A recent study (ref. (10)) provides an explanation for the origin of the relative angular misalignment and suggests that the natural primary-seal configuration is one of angular misalignment because of secondary seal friction and inertia of the primary-ring.

The relative angular misalignment model is shown in fig. 8. The seat is stationary and has an angular misalignment with respect to the centerline of the rotating shaft. The primary ring rotates with the shaft. (A rotating seat configuration introduces primary-ring inertia forces.) The primary ring has axial flexibility and also is free to align itself with the seat face. These degrees of freedom are duplicated by allowing angular oscillation of the primary ring about the Y- and Z-axes (fig. 8) with their origin at the center of mass. In the third mode of freedom the seal is free to translate along the X-axis. Parallel eccentricity is not considered since it is assumed to have no significant effect on load support.

In order to explain the model (fig. 8), the coordinate system (X,Y,Z) is fixed in space and located

at the center of mass of the primary ring. The centerline of the rotating shaft lies along the X-axis and the centerline of the primary ring is inclined at a small angle (β) to the X-axis. A separate cylindrical coordinate system with its origin on the centerline and with the r,θ -plane coincident with the non-rotating surface is used to calculate the hydrodynamic pressures.

Additional details of the mathematical model are shown in fig. 9, in which the response of the primary ring to seat angular misalignment α is illustrated. It is postulated that the primary ring has an angular misalignment position between the limiting positions indicated in fig. 9. These limiting positions are (1) a primary-ring alignment perpendicular to the shaft centerline ($\beta = 0$) and (2) an alignment parallel to the seat face ($\beta = \alpha$ and $\beta = \alpha$). In practice the primary-ring face will probably assume a position between the two extremes. (Note that β is equal to or less than α .)

Of interest in this model is the misalignment of the faces in a circumferential direction. The variation of seal-gap height h in the circumferential direction is, in effect, an inclined slider bearing having a converging gap over 180° of arc and a diverging gap in the remaining 180° . This circumferential incline is the source of load support. However, the effect of this angular misalignment on load support in the radial direction is small, and h can be assumed to be constant in the radial direction.

The forces considered in the model of seal operation are (1) the hydrodynamic and shear forces generated in the fluid film, (2) a distributed spring force, and (3) a distributed force from the secondary seal acting against the primary ring motion.

The force generated by the fluid film can be determined by the Reynolds equation in the short-bearing form (ref. (11)), with the restriction that pressure is positive in the converging portion and ambient in the diverging portion. The spring force may be assumed to be equally distributed with constant magnitude since the seal displacements of interest are only of the order of 0.1 millimeter (0.004 in.) or less. The secondary-seal external friction, internal hysteresis or elastic displacement (damping) forces on the converging gap at any one instant are directed in a positive X-direction and these forces on the diverging side are directed in a negative X-direction. Reference to fig. 9 helps to clarify the direction in which the forces act. For the rotation direction indicated, any point on the primary ring that is on the converging side is moving in a negative X-direction, and the secondary-seal friction opposes this motion. The opposite is true for the diverging portion.

These frictional forces can be approximated by a distributed force acting along a mean diameter of the secondary ring. Figure 9 illustrates this frictional resistance. (Note that a change in sign occurs when the X,Z-plane passes through the maximum and minimum film thicknesses.) Since the seal radius is usually large compared to the radial dam width, some of the analysis involving the seal dam and the secondary seal can be based on the same characteristic (mean) seal radius R without introducing significant error. This simplifies the calculations. For a detailed treatment of this model the reader is referred to ref. (10).

A large number of possible primary-seal configurations can be devised using waviness and angular misalignment (fig. 6(a) and (b)). Some of these were considered in ref. (11), and these are:

- (1) Relative angular misalignment
 - (a) non-rotating primary ring

- (b) rotating primary ring
- (2) Waviness in rotating primary-ring
- (3) Waviness in nonrotating primary-ring
- (4) Combined angular misalignment and primary-ring waviness

- (a) nonrotating primary ring
- (b) rotating primary ring

The possible configurations proliferate as other primary-seal geometries are introduced (fig. 6). Further, the sealed pressure could be at either the outer diameter or the inner diameter of the seal, and both faces could be rotating at different speeds. A group of complex configurations can be formulated by introducing waviness into the seat as well as into the primary ring. These complex configurations, waviness in the seat, plus waviness in the primary ring, plus relative angular misalignment, introduce complex pressure patterns.

Lubrication, Hydrostatic Effects

The hydrostatic force in the primary-seal becomes increasingly critical in regard to lubrication and wear as the pressure increases, and the effect of hydrostatic force on seal stability has only been recently recognized (ref. (21)). In this study of ref. (21), an analysis was made of axial force, tilting moment, and leakage over a range from zero to full angular misalignment (surfaces touching). The study revealed that the angular misalignment causes a non-axisymmetric hydrostatic pressure pattern and when the high pressure is on the O.D. of the primary face, both axial force and angular moment are nonrestoring. However, with the pressure on the I.D. of the primary-seal, the seal is stable.

With regard to seal stability, the illustrations in Table III show several possibilities including the angular misalignment case discussed above. The first case illustrated is that of parallel surfaces; with high pressure at either the O.D. or the I.D., the primary seal has an axisymmetric pressure pattern and the axial film stiffness and angular righting moment are both zero. Axisymmetric coning deformations (cases b and c) are equivalent, the controlling factor being the location of the high pressure with respect to the coning. If the coning results in a divergent channel to leakage flow, then film stiffness is negative and both the axial force and moment tilting moment are nonrestoring. On the other hand, if the high pressure is located such that the leakage channel is converging, then both the axial force and tilting moment are restoring.

The situation becomes complex when there is combined coning and angular misalignment (cases e and f), with an important parameter being the magnitude of the coning with respect to the angular misalignment.

Requirements for Stable Operation

The preceding discussions suggest that seal lubrication is a complex mechanism involving many possible primary-seal geometries, liquid vaporization, hydrodynamic forces, hydrostatic forces, inertia and secondary seal friction. However complex, certain conditions must be met for liquid film lubrication, and these are:

(1) Balance of Axial Forces - The pressure in the fluid film (opening force) must equal the closing force. With reference to fig. 10, the closing force is the spring force plus the sealed pressure acting on an annular area from the O.D. of the secondary seal to the O.D. of the primary-ring. (This case of sealed pressure at the primary-ring O.D. illustrates the gen-

eral principle.) In fig. 10(a), the area over which the sealed pressure acts is quite large, being equal to the area of the primary-seal; this is an unbalanced seal, (which was described in the companion paper, ref. (12)) because the closing force is apparently greater than the opening force for an assumed linear pressure drop. In actuality, for film lubrication to prevail the pressure profile in the primary seal cannot be linear because of beneficial hydrodynamic forces, hydrostatic forces and vaporization effects; the seal opening and closing forces will be balanced.

The closing force can be reduced by decreasing the area over which the sealed pressure acts, this is illustrated in fig. 10(b), and is commonly called a balance seal. In this regard, in the context of this paper the terms "balanced" and "unbalanced" have meaning only in that, in a balanced seal, some attempt has been made to reduce the magnitude of the closing force.

The crux of the problem lies in avoiding selection of a closing force too high such that film lubrication cannot be achieved, and at the same time avoiding selection of a closing force too low such that a face distortion or phase change will cause the opening force to exceed the closing force.

(2) Positive Axial Film Stiffness - A positive film stiffness is required for stable operation, that is, if the closing force increases for some reason (shock load, etc.), then an increase in opening force accompanies any decrease in film thickness.

(3) Balance of Moments - The restoring moment generated by the film must be sufficient to balance the moments due to secondary seal friction, hydrostatic forces, etc.

Example: Seal Pressure Balance and Operating Film Thickness

The seal analyzed by ref. (14) can be used to illustrate the effect of pressure balance on the operating modes. The seal dimensions and operating conditions are given in fig. 11; the sealed fluid is water. Figure 11(a) illustrates a balanced seal in which the secondary seal diameter has been selected to provide a closing force of 32 pounds; the total closing force being 42 pounds (10 lb spring force). A full liquid film across the sealing dam has a linear pressure drop, and its associated opening force is 40 pounds (for the conditions given in fig. 11). Thus, this balanced seal would tend to operate in a full liquid film mode (unless shear heating was high enough to induce a phase change).

However, certain other conditions are required for seal stability as previously noted. One of these is a positive axial film stiffness, and since parallel faces have zero hydrostatic stiffness, the positive stiffness, for this full liquid film case, must be provided by hydrodynamic forces (e.g., waviness) or by convergent faces (e.g., mechanical or thermal distortion, see table III). Also, stable operation requires a restoring moment capability to resist overturning moments, and for the seal illustrated in fig. 11(a), this would have to be provided by hydrostatic forces (see ref. (21)) and by hydrodynamic effects (see ref. (11)).

On the other hand, if the secondary seal diameter is designed to provide an "unbalanced" seal, say closing force area A_2 equals primary-seal area A_1 , then the total closing force is 356.3 N (80.1 lb). Using the analysis of ref. (14) as given in fig. 12, the operating film thickness is 2.25 μm (90×10^{-6} in.) and the liquid is vaporizing very near the outer edge. An important consequence is that this vaporization causes a large decrease in leakage flow as compared to the

full liquid film case. As can be determined from fig. 12, vaporization provides a positive axial film stiffness and a positive moment stiffness; these are needed for stable operation.

Seal Lubrication Models

Table IV summarizes some of the possible full fluid film operating modes. The first types are characterized by a liquid film which exists across the primary-seal from the I.D. to the O.D. This lubrication mode is probably most common in low speed applications and lubrication is due to hydrodynamic or hydrostatic effects. In applications having very low pressure differentials, hydrostatic effects are not significant and the seal opening force must be generated by hydrodynamic effects (model 1(a)) (these have been reviewed by ref. (11)); when significant pressure differentials prevail, the seal achieves its opening force through a combined hydrostatic and hydrodynamic effect (model 1(b)).

Moderate to high speed can induce vaporization of the liquid in the primary seal, and as discussed previously, this can produce beneficial effects in regard to opening force, film stiffness and leakage. It should be noted that vaporization can be a sole means of generating effective opening forces (model 2(a)). The range of stable films is illustrated in fig. 13 for the two examples analyzed by ref. (14).

The most probable operating mode for a large class of seals operating at moderate to high speed is the fourth case (model 2(b)) illustrated in Table IV, and this is vaporization combined with hydrodynamic and hydrostatic effects. Because of the moderate to high speeds the vaporization occurs near the entrance, hence, by itself may not provide positive film stiffness, in fact, the film stiffness may be negative; film collapse and rubbing contact are prevented by hydrostatic and hydrodynamic effects.

CONCLUDING REMARKS

It should be emphasized that seal life and leakage are intimately dependent upon lubrication, the lubricant being the sealed fluid. As indicated in the preceding discussion, seal lubrication, in general, is not well understood and viable lubrication models will have to be formulated before predictions regarding leakage and life can be modeled. However, prior studies cited have provided valuable insight into the lubrication mechanisms.

Some classes of seal apparently operate with a fluid film separating the faces of the primary seal; and within this general class of lubrication it is postulated that there are four different modes of lubrication. These are:

Liquid Film Forces

- (a) hydrodynamic due to waviness and angular misalignment (low pressure)
- (b) combined hydrodynamic and hydrostatic (low speed, moderate to high pressures)

Liquid/Vapor Film Forces

- (a) thermally induced phase change
- (b) thermally induced phase change combined with hydrodynamic and hydrostatic forces

The discussion also pointed out the fact that the lubricating film thickness was very small (in the range of 1 micron) and therefore small variations in the primary seal geometry had a dramatic effect on the lubricating process. In general, these small variations in primary seal geometry are due to unplanned effects of thermal gradients, pressure dis-

tortions, wear, etc.; these effects complicate construction of seal performance models.

It was also mentioned that primary-seal ring inertia (due to mating ring runout) and secondary seal friction are significant factors in seal performance, and, in general, these are not included in published seal performance models. Finally it should be noted that refs. (14) and (21) contain computer programs which permit analysis of thermal and hydrostatic effects on seal stability.

REFERENCES

1. Sneek, H. J., "The Misaligned, Eccentric Face Seal," Preprint 15A, Am. Soc. Lubri. Engrs., May 1969.
2. Hamilton, D. B., Walowit, J. A., and Allen, C. M., "A Theory of Lubrication by Microirregularities," Journal of Basic Engineering, Trans. ASME, Vol. 88, Mar. 1966, pp. 177-185.
3. Nau, B. S., "Hydrodynamics of Face Seal Films," Proceedings of the Second International Conference on Fluid Sealing, B.S. Nau, H. S. Stephens, and D. E. Turnbull, eds., British Hydromechanics Research Assoc., England, 1964, pp. F5-61 to F5-80.
4. Golubiev, A. I., "On the Existence of a Hydraulic Film in Mechanical Seals," Proceedings of the Third International Conference on Fluid Sealing, A. L. King, B. S. Nau, and H. S. Stephens, eds., British Hydromechanics Research Assoc., England, 1961, E1-1 to E1-8.
5. Stanghan-Batch, B. and Iny, E. H., "A Hydrodynamic Theory of Radial-Face Mechanical Seals," Journal of Mechanical Engineering Science, Vol. 15, Feb. 1973, pp. 17-24.
6. Pape, J. G., "Fundamental Research on a Radial Face Seal," American Society of Lubrication Engineers Transacting, Vol. 11, Oct. 1968, pp. 302-309.
7. Iny, E. H., "A Theory of Sealing with Radial Face Seals," Wear, Vol. 18, 1971, pp. 51-69.
8. Haardt, R. and Godet, M., "Axial Vibration of a Misaligned Radial Face Seal under a Constant Closure Force," Preprint 74AM-7D-1, Am. Soc. Lubri. Engrs., Apr.-May 1974.
9. Kojabashian, C. and Richardson, H. H., "A Micro-pad Model for the Hydrodynamic Performance of Carbon Face Seals," Proceedings of the Third International Conference on Fluid Sealing, A. L. King, B. S. Nau, and H. S. Stephens, eds., British Hydromechanics Research Assoc., England, 1967, pp. E4-41 to E4-71.
10. Ludwig, L. P. and Allen, G. P., "Face-Seal Lubrication. II - Theory of Response to Angular Misalignment," NASA TN D-8102, Mar. 1976.
11. Ludwig, L. P., "Face-Seal Lubrication. I - Proposed and Published Models," NASA TN D-8101, Apr. 1976.
12. Ludwig, L. P. and Greiner, H. F., "Design Considerations in Mechanical Face Seals for Improved Performance - I Basic Configurations," NASA TM X-73735, Aug. 1977.

13. Orcutt, F. K., "An Investigation of the Operation and Failure of Mechanical Face Seals," *Journal of Lubrication Technology*, Trans. ASME, Vol. 91, Oct. 1969, pp. 713-725.
14. Birchak, Michael; and Hughes, W. F., Simplified Computer Program for the Analysis of Phase Change in Liquid Face Seals, NASA CR-134668, 1977.
15. Mayer, E., "Thermodynamics in Mechanical Seals," Proceedings of the Fourth International Conference on Fluid Sealing, A. L. King, B. S. Nau, and H. S. Stephens, eds., British Hydromechanics Research Assoc., England, 1970, pp. 124-128.
16. Mayer, E., "High Duty Mechanical Seals for Nuclear Power Stations," Proceedings of the Fifth International Conference on Fluid Sealing, A. L. King, B. S. Nau, and H. S. Stephens, eds., British Hydromechanics Research Assoc., 1971, pp. A5-37 to A5-47.
17. Banerjee, B. N. and Burton, R. A., "An Instability for Parallel Sliding of Solid Surfaces Separated by a Viscous Liquid Film," Preprint 75-Lub-4, Am. Soc. Mech. Engrs., Oct. 1975.
18. Lebeck, A. O., "Waviness Distortion and Wear In Mechanical Face Seals." New Mexico University Report ME-64(74) NSF-271-1, Dec. 1974.
19. Ishiwata, H. and Hirabayashi, H., "Friction and Sealing Characteristics of Mechanical Seals," Proceedings of the International Conference on Fluid Sealing, British Hydromechanics Research Assoc., 1961, Paper D-5.
20. Summers-Smith, D., "Laboratory Investigation of the Performance of a Radial Face Seal," Proceedings of the International Conference on Fluid Sealing, British Hydromechanics Research Assoc., 1961, Paper D-1.
21. Etsion, I., "Nonaxisymmetric Incompressible Hydrostatic Pressure Effects in Radial Face Seals," NASA TN D-8343, Nov., 1976.

TABLE I. - MATHEMATICAL MODELS FOR SURFACE WAVINESS AND MISALIGNMENT AS SOURCES OF PRESSURE GENERATION BETWEEN PRIMARY-SEAL SURFACES

Source of pressure generation	Restrictions	Governing equations	Solution technique	Pressure distribution equation	Reference
Angular misalignment of one face	No axial motion; constant centerline film thickness; cylindrical coordinates attached to rotating face	$\frac{\partial p}{\partial r} = \frac{\rho u^2}{r} + \mu \frac{\partial^2 v}{\partial z^2}$ $\frac{\partial p}{\partial z} = \frac{\partial^2 u}{\partial z^2} = 0$ <p>Assumed input data: (1) Film thickness (2) Angular misalignment (3) Eccentricity</p>	Governing equations solved explicitly for pressure, torque, leakage rate, and separating force	$p = 6\mu [\epsilon \Omega \sin(\phi - \theta)] \int_{R_0}^r \frac{dr}{h^2} + 6\mu [\omega \cos \gamma \tan^2 \gamma \sin \theta \cos \theta] \int_{R_0}^r \frac{r dr}{h^2}$ $+ \frac{\rho r^2}{2} \left[\omega \Omega \cos \gamma + \frac{3}{10} (\omega \cos \gamma - \Omega)^2 \right] + 12\mu \phi(\theta) \int_{R_0}^r \frac{dr}{rh^3} + \Psi(\theta)$ $+ 2\mu (\omega \cos \gamma + \Omega) \sin \theta \tan \gamma \int_{R_0}^r \frac{r^2 dr}{h^3}$ <p>where $\Psi(\theta) = p_0$, Ω is angular velocity of the eccentric surface, $h = h_0 - r \cos \theta \tan \gamma$, and</p> $\phi(\theta) = \frac{1}{12\mu \int_{R_0}^{R_1} \frac{dr}{rh^3}} \left\{ p_1 - p_0 - 6\mu [\epsilon \Omega \sin(\phi - \theta)] \int_{R_0}^{R_1} \frac{dr}{h^2} \right.$ $- 6\mu (\omega \cos \gamma \tan^2 \gamma \sin \theta \cos \theta) \int_{R_0}^{R_1} \frac{r dr}{h^2} + \frac{\rho}{2} (R_0^2 - R_1^2)$ $\times \left[\Omega \omega \cos \gamma + \frac{3}{10} (\omega \cos \gamma - \Omega)^2 \right] - 2\mu (\omega \cos \gamma + \Omega)$ $\times \sin \theta \tan \gamma \int_{R_0}^{R_1} \frac{r^2 dr}{h^3} \left. \right\}$	3
Angular misalignment (also admits waviness and axial vibration)	Constant centerline film thickness; cylindrical coordinates	$\frac{\partial}{\partial r'} \left(r'^3 \frac{\partial p'}{\partial r'} \right) + \frac{\partial}{\partial \theta} \left(\frac{h'^3}{r'} \frac{\partial p'}{\partial \theta} \right) = -r'^2 [\cos(\theta - \Omega) + x' \cos \theta]$ <p>where $\Omega = \omega t$ Nondimensional form of Reynolds equation</p>	Finite difference technique, used for solution of pressure	Nondimensional symbols: $r' = r/R$ $h' = h/h_0$ $p' = \frac{h_0^3}{6\mu R^3 \omega \beta} (p - p_0)$ $x' = \frac{\alpha}{\beta}$	12
	Constant axial load	$\frac{\partial}{\partial r'} \left(r'^3 \frac{\partial p'}{\partial r'} \right) + \frac{\partial}{\partial \theta} \left(\frac{h'^3}{r'} \frac{\partial p'}{\partial \theta} \right) = -r'^2 [\cos(\theta - \Omega) + x' \cos \theta]$ $+ \frac{2h_0}{R\omega\beta} \frac{\partial \lambda}{\partial t}$ <p>Nondimensional form of Reynolds equation; $\lambda(t)$ describes squeeze-film motion</p>	Trial and error procedure, used to find specific cases of film-thickness function $\lambda(t)$ which give a constant load		

E-9238-2

Angular misalignment of both faces	Cylindrical coordinates; Reynolds equation, time-dependent, constant axial load; short-bearing approximation, fixed misalignment	$\frac{\partial}{\partial r} \left(r \frac{h^3}{\mu} \frac{\partial p}{\partial r} \right) = -6r^2 \omega [\beta \cos(\theta - \omega t) + \alpha \cos \theta] + 12r \frac{\partial h(t)}{\partial t}$	Numerical methods	13
Angular misalignment and surface waves in a circumferential direction	Cylindrical coordinates; Reynolds equation for two dimensions; fixed misalignment	$r \frac{\partial}{\partial r} \left(\frac{r \rho h^3}{12\mu} \frac{\partial p}{\partial r} \right) + \frac{\partial}{\partial \theta} \left(\frac{\rho h^3}{12\mu} \frac{\partial p}{\partial \theta} \right) = \frac{\partial}{\partial \theta} \left(\rho \frac{\omega r^2 h}{2} \right)$	Assumed form of pressure solution	6
Surface waves in a circumferential direction	Cylindrical coordinates; simplified momentum equation; constant centerline film thickness	$\frac{\partial p}{\partial r} = \rho \frac{v^2}{r} + \mu \frac{\partial^2 v}{\partial z^2}$ $\frac{\partial p}{\partial z} = \frac{\partial^2 u}{\partial z^2} = 0$ <p>Continuity equation:</p> $\frac{\partial}{\partial r} \left(\int_0^{-h} u \, dz \right) + \int_0^{-h} \frac{\partial v}{\partial \theta} \, dz = 0$	Governing equations, solved explicitly for pressure, torque, leakage rate, and separating force	4
Two waves in circumferential direction combined with angular misalignment	Cylindrical coordinates; Reynolds equation with short-bearing approximation	$\frac{1}{r} \frac{\partial}{\partial r} \left(h^3 r \frac{\partial p}{\partial r} \right) = 6\mu \omega \frac{\partial h}{\partial \theta}$	Reynolds equation solved explicitly for pressure	11
Circumferential waves	Rectangular coordinates; Reynolds equation; short-bearing approximation	$h^3 \frac{\partial^2 p}{\partial y^2} = 6\mu U \frac{\partial h}{\partial x}$	Reynolds equation solved explicitly for pressure	21
Circumferential waves	Cylindrical coordinates; Reynolds equation in two dimensions and time dependent	$\frac{1}{r^2} \frac{\partial}{\partial \theta} \left(\frac{h^3}{12\mu} \frac{\partial p}{\partial \theta} \right) + \frac{\partial}{\partial y} \left(\frac{h^3}{12\mu} \frac{\partial p}{\partial y} \right) = \frac{\omega}{2} \frac{\partial h}{\partial \theta} + \frac{\partial h}{\partial t}$	Finite difference method of solution of Reynolds equation in nondimensional form	10

$$p = \left[\alpha \varphi_1(r, \theta) + \alpha^2 \varphi_2(r, \theta) + O(\alpha^2) \right]$$

where

φ_1, φ_2 first two pressure coefficients

$$p - p_0 = \frac{3}{20} \rho \omega^2 (r^2 - R_0^2) + \frac{6\mu \omega \epsilon}{h^2} \sin(\phi - \theta)(r - R_0)$$

$$+ \frac{3}{2} \frac{\mu \omega}{h^3} (r^2 - R_0^2) \frac{\partial h}{\partial \theta} + \frac{\ln \left(\frac{r}{R_0} \right)}{\ln \left(\frac{R_1}{R_0} \right)} \left\{ P_1 - P_0 - \frac{3}{20} \rho \omega^2 (R_1^2 - R_0^2) \right\}$$

$$- \frac{3}{2} \frac{\mu \omega}{h^3} (R_1^2 - R_0^2) \frac{\partial h}{\partial \theta} - \frac{6\mu \epsilon \omega}{h^2} \sin(\phi - \theta)(R_0 - R_1)$$

$$p = \frac{1}{\ln \left(\frac{R_0}{R_1} \right)} \left\{ \gamma P_S + \frac{3\mu \omega}{2h^3} \frac{dh}{d\theta} \left[r^2 \ln \left(\frac{R_0}{R_1} \right) - R_1^2 \ln \left(\frac{r}{R_1} \right) - R_1^2 \ln \left(\frac{R_0}{r} \right) \right] \right\}$$

$\gamma = \ln(R_0/r)$ for inside seal, and $\ln(r/R_1)$ for outside seal

$$p = 3\mu U \frac{1}{h^3} \frac{\partial h}{\partial x} \left[y^2 - \frac{(R_0 - R_1)^2}{4} \right]$$

TABLE II. - MATHEMATICAL MODELS FOR LOAD CAPACITY OR PRESSURE GENERATION IN PRIMARY-SEAL SURFACES

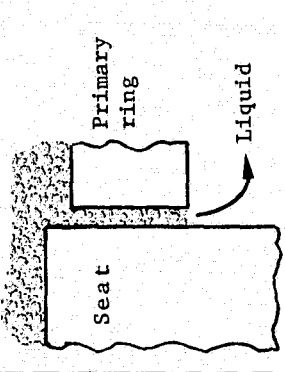
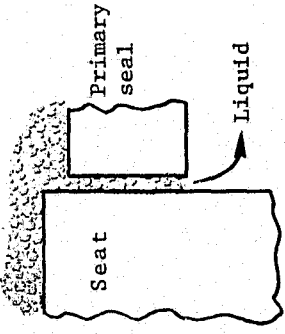
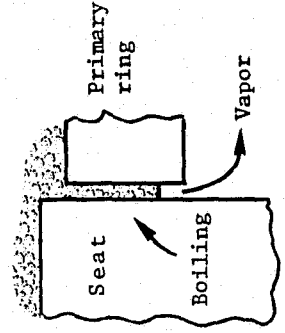
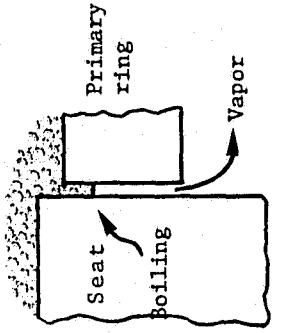
Source of pressure generation	Restriction	Governing equations	Solution technique	Pressure distribution equation	Reference
Micropads produced by "run in" wear, which act as small, inclined slider bearings	Assumes each pad is a small, rectangular step bearing		Closed form; observed statistical distribution of pads used	$\bar{p}_b = 2\rho\mu Ub \frac{\delta}{(h_2 + \delta)^3 + h_2^3}$ <p>where</p> $\rho = \frac{96}{\pi^4} \bar{L}^2 \sum_{N=1,3,5,\dots} N^{-4} \tanh \frac{\pi N}{4L} \tanh \frac{\pi N}{2L}$ <p>and</p> <p>N variable of summation \bar{p}_b average hydrodynamic pressure 2b circumferential length of micropad δ pad height h_2 minimum clearance L radial width of pad \bar{L} aspect ratio, L/2b</p>	14
Surface asperity tops, which act as small inclined slider bearings	Reynolds equation - two-dimensional form, rectangular coordinates	$\frac{\partial}{\partial x} \left(h^3 \frac{\partial p}{\partial x} \right) + \frac{\partial}{\partial y} \left(h^3 \frac{\partial p}{\partial y} \right) = -6\mu \frac{U}{R_o} (h_0 - h_m)$	Nondimensional form - expansion of dimensionless pressure in series solution	$\bar{p} = \frac{3}{4} \frac{\mu UR_o \delta}{h_0^3}$ <p>where</p> <p>$\delta = h_0 - h_2$ and</p> <p>\bar{p} average pressure h_0 average film thickness h_m minimum film thickness R_o asperity radius</p>	5
Small, inclined slider bearings produced by thermal deformation around microleakage channels in primary seal face	Rectangular coordinates; pressure as a function of velocity in the circumferential direction	$\frac{\partial p}{\partial x} = \mu \frac{\partial^2 u}{\partial z^2}$ $\frac{\partial u}{\partial x} + \frac{\partial v}{\partial y} = 0$ $u \frac{\partial T}{\partial x} = \frac{\lambda}{c\rho} \frac{\partial^2 T}{\partial z^2} + \frac{\mu}{c\rho J} \left(\frac{\partial u}{\partial z} \right)^2$ $\mu = \mu(T)$ $\frac{\partial^2 T}{\partial x^2} + \frac{\partial^2 T}{\partial z^2} = 0$ $\delta(h) = -\alpha \int_0^\Delta [T(x + \delta x, z) - T(x, z)] dz$ $h = h(x)$	(1) Method of relaxation, used to solve the seven governing equations (2) (3) (4) (5) (6) (7)	$\bar{p} = \frac{2}{5\pi} \left(\frac{\alpha l^3 \mu^2 U^2}{J c \rho h^5} \right)$ <p>where</p> <p>\bar{p} average pressure α coefficient of linear expansion l distribution between scratches J mechanical equivalent of heat c specific heat</p>	7

E-9298-2

TABLE III. - SEAL STABILITY MODELS

		Liquid film		
		Pressure pattern	Axial stiffness	Restoring moment
A. Parallel	$P_0 < P_1$ $P_0 > P_1$	Axisymmetric Axisymmetric	Zero Zero	Zero Zero
B. Coned	$P_0 < P_1$ $P_0 > P_1$	Axisymmetric Axisymmetric	Negative Positive	Negative Positive
C. Coned	$P_0 < P_1$ $P_0 > P_1$	Axisymmetric Axisymmetric	Positive Negative	Positive Negative
D. Misaligned	$P_0 < P_1$ $P_0 > P_1$	Nonaxisymmetric Nonaxisymmetric	Positive Negative	Positive Negative
E. Coned and misaligned	$P_0 < P_1$ $P_0 > P_1$	Nonaxisymmetric Nonaxisymmetric	Negative Positive	Negative Positive
F. Coned and misaligned	$P_0 < P_1$ $P_0 > P_1$	Nonaxisymmetric Nonaxisymmetric	Positive Negative	Positive Negative

TABLE IV. - MECHANISM OF GENERATING OPENING FORCE FOR SEAL OPERATING ON FLUID FILMS

Liquid films (model 1)		Liquid/Vapor films (model 2)	
<p>Hydrodynamic (Model 1(a))</p> <p>(a) Wavy and misaligned primary-seal faces</p> <p>(b) Model applies to seals with very low pressure differentials</p> <p>(c) Model requires cavitation in divergent regions</p>	<p>Combined hydrodynamic and hydrostatic (Model 1(b))</p> <p>(a) Wavy and misaligned primary-seal faces</p> <p>(b) Model applies to seals with moderate to high pressure differentials and low speeds</p>	<p>Thermal (Model 2(a))</p> <p>(a) Parallel primary-seal faces</p> <p>(b) Model applies to seal with sufficient shear heating to cause film phase change to occur near exit of primary-seal; moderate speeds</p>	<p>Combined thermal with hydrodynamic and hydrostatic effects</p> <p>(a) Wavy and misaligned primary-seal faces</p> <p>(b) Model applies to seal with shear heating high enough to cause film phase change to occur near entrances of primary-seal; high speeds</p>
			

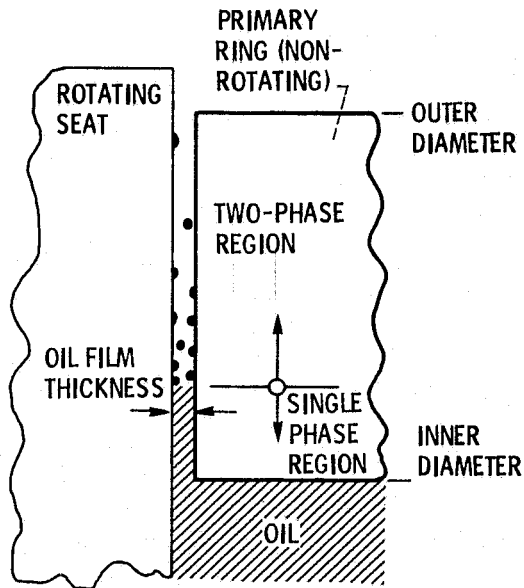


Figure 1. - Conventional oil-lubricated radial face seal. Seal sliding velocity, 11.3 m/sec (37 ft/sec). (From ref. 13.)

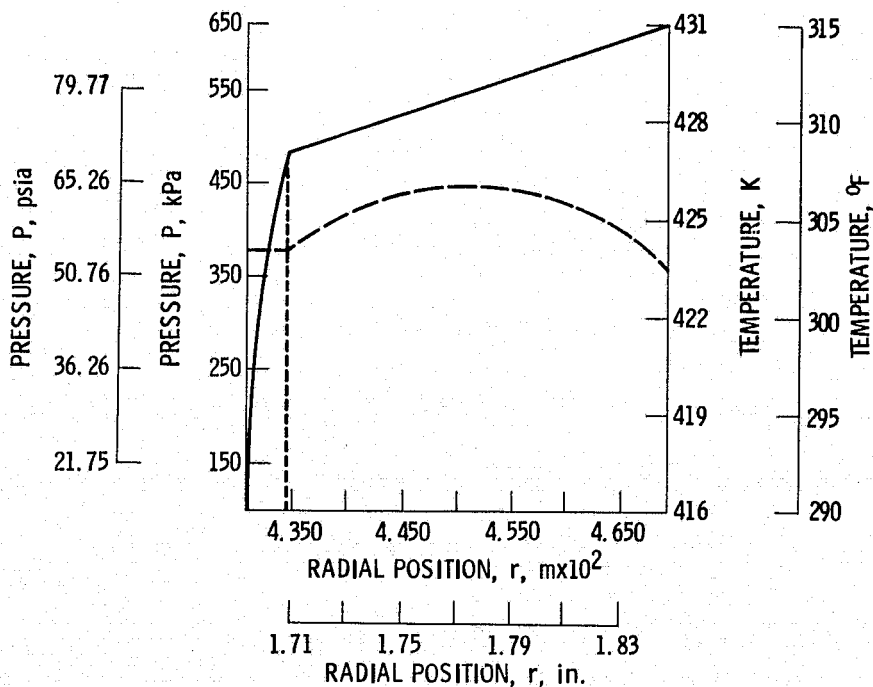


Figure 2. - Temperature and pressure distribution in the film space. $P_1 = 15.0$ psia (103.4 kPa), $P_2 = 90.0$ psia (620.4 kPa), $r_1 = 1.693$ inches (0.04300 m), $r_2 = 1.849$ inches (0.04696 m), $h = 50.0 \times 10^{-6}$ inches (1.27×10^{-6} m), $\omega = 7200$ rpm (754 rad/s), $k = 26$ Btu/hr-ft- $^{\circ}F$ (45 W/m-K). (From ref. 14.)

E-1298-2

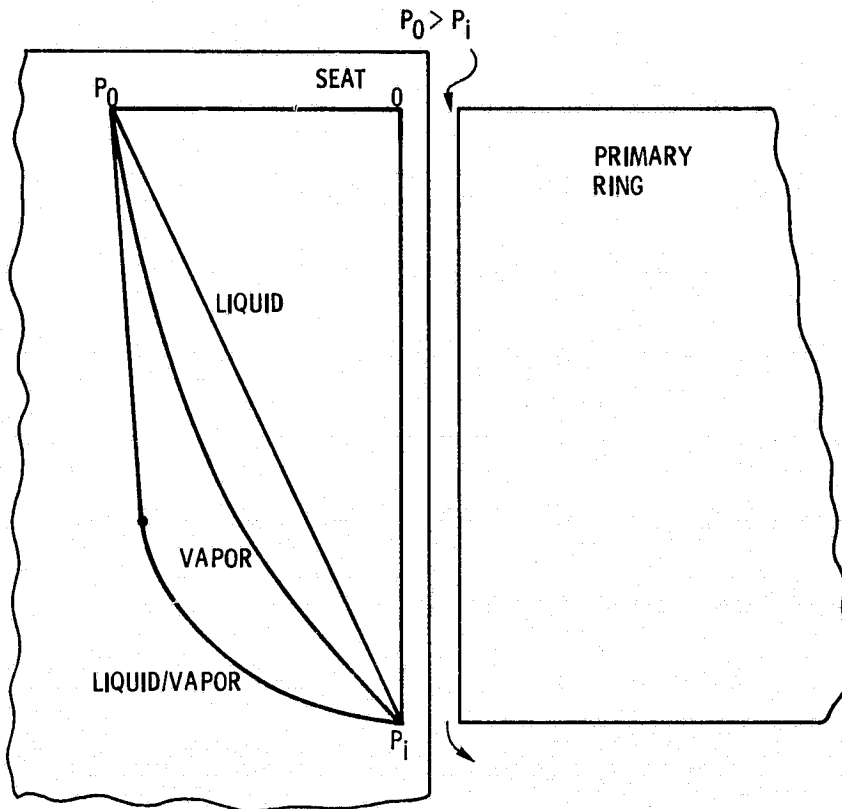


Figure 3. - Pressure gradients for liquid, vapor, and liquid/vapor conditions in the primary-seal.

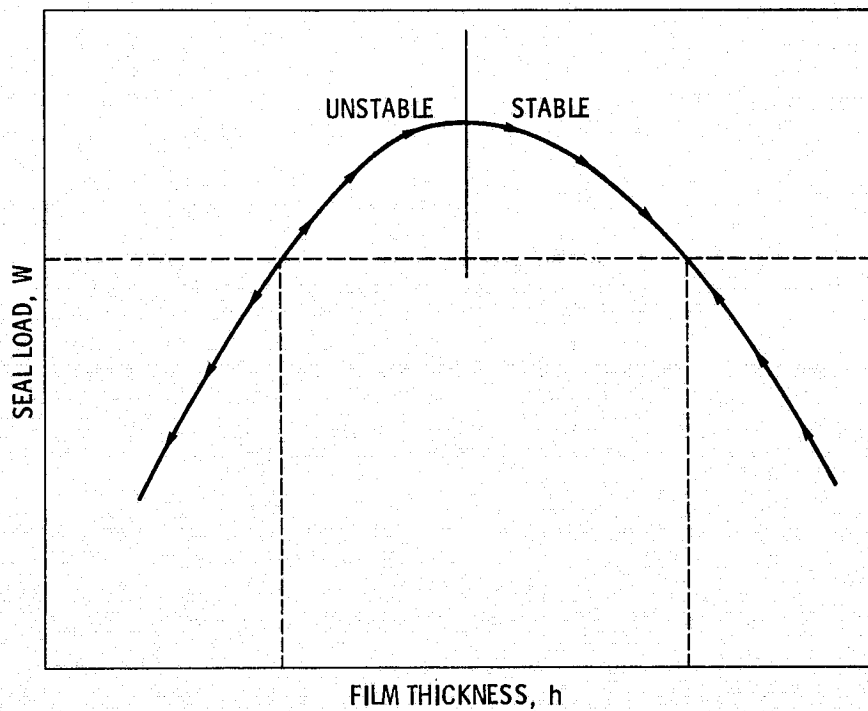


Figure 4. - Effect of film thickness on seal instability. (From ref. 14.)

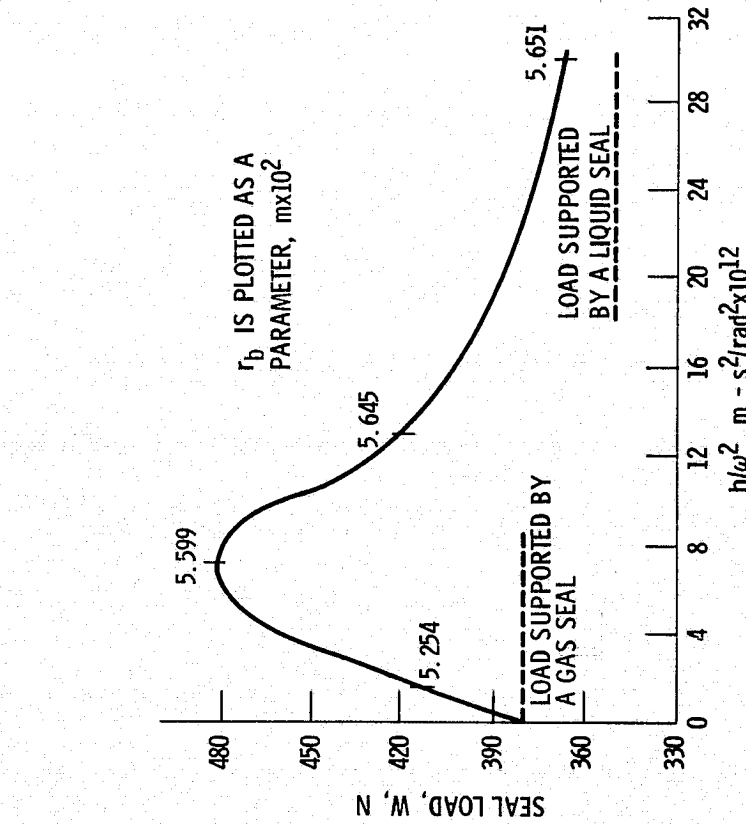


Figure 5. - Effect of h/ω^2 on the seal load. $P_1 = 45.0$ psia (310.2 kPa), $P_2 = 15.0$ psia (103.4 kPa), $r_1 = 2.025$ inches (0.05144 m), $r_2 = 2.225$ inches (0.05652 m), $k = 7.5$ Btu/hr-ft- $^{\circ}$ F (13 W/m-K), $T_{\infty} = 205^{\circ}$ F (369 K). (From ref. 14.)

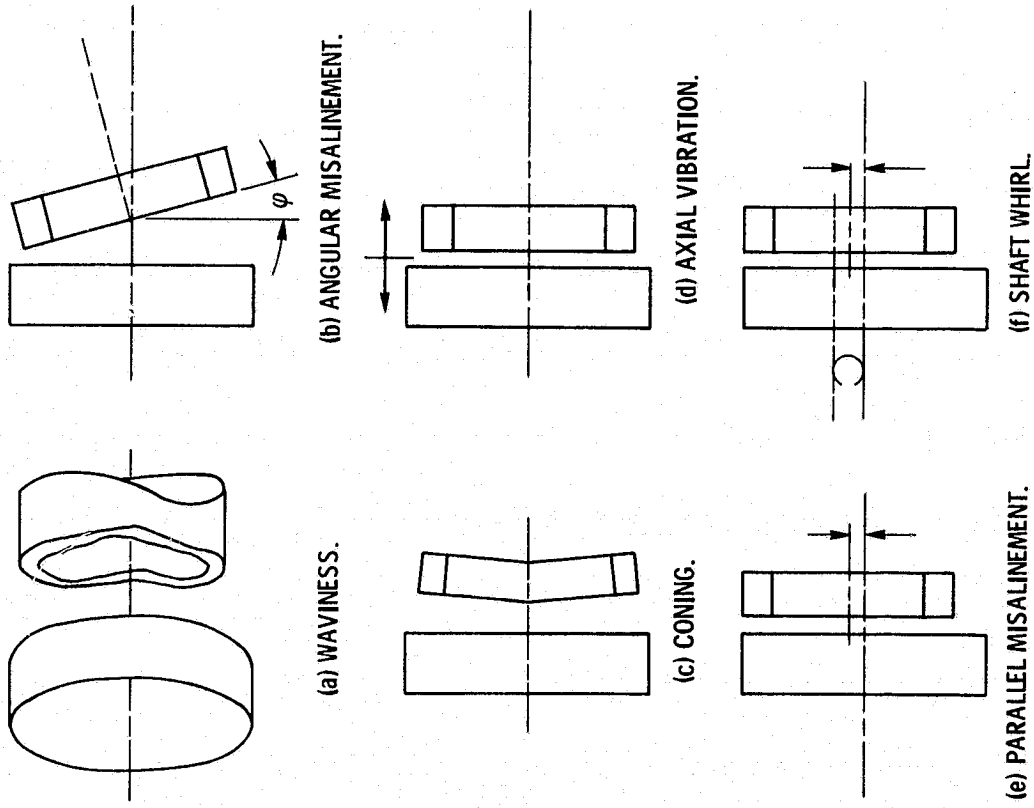


Figure 6. - Possible primary-seal geometries.

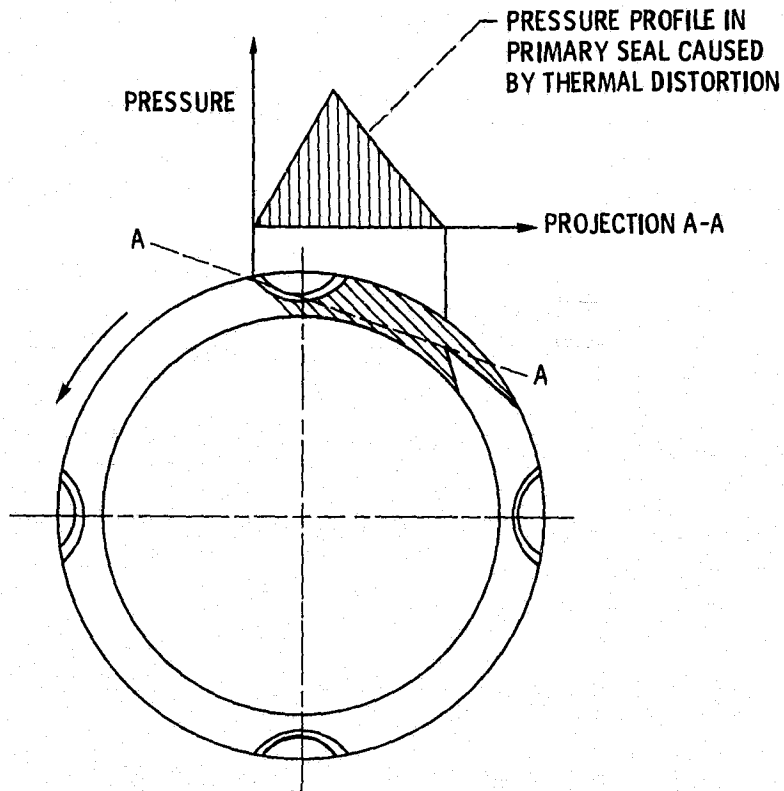


Figure 7. - Circular grooves in face of primary ring. (From ref. 16.)

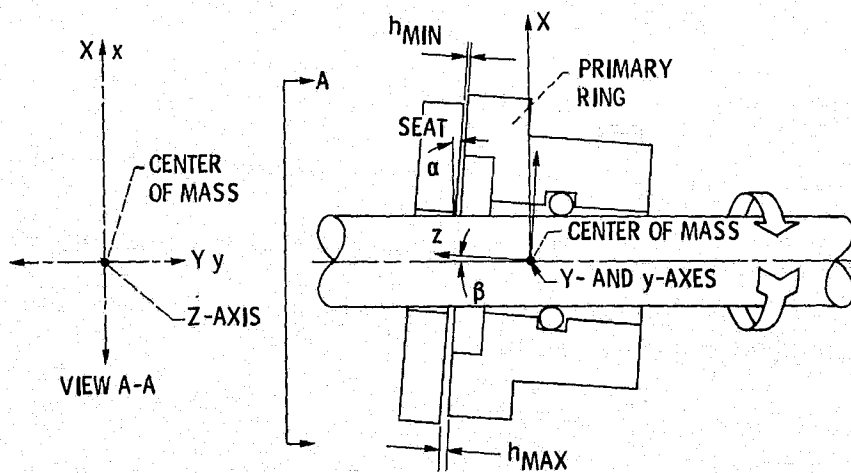


Figure 8. - Mathematical model of radial face seal with rotating primary ring.

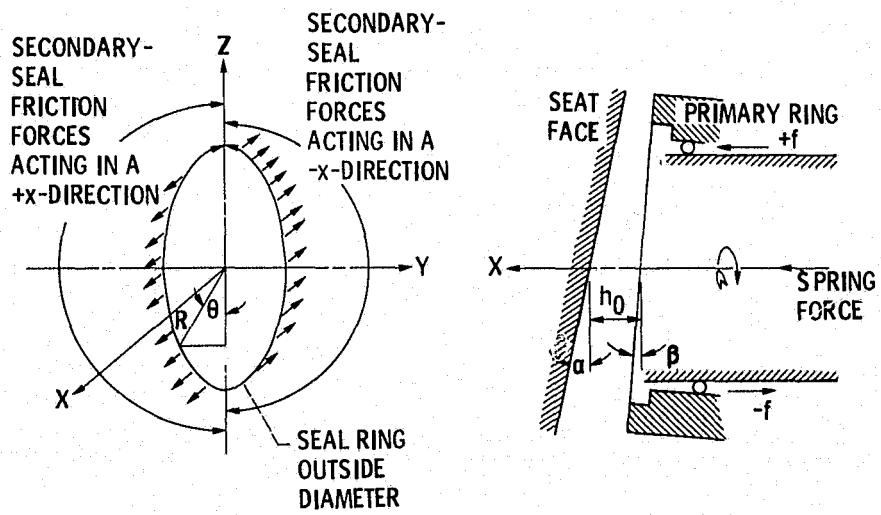
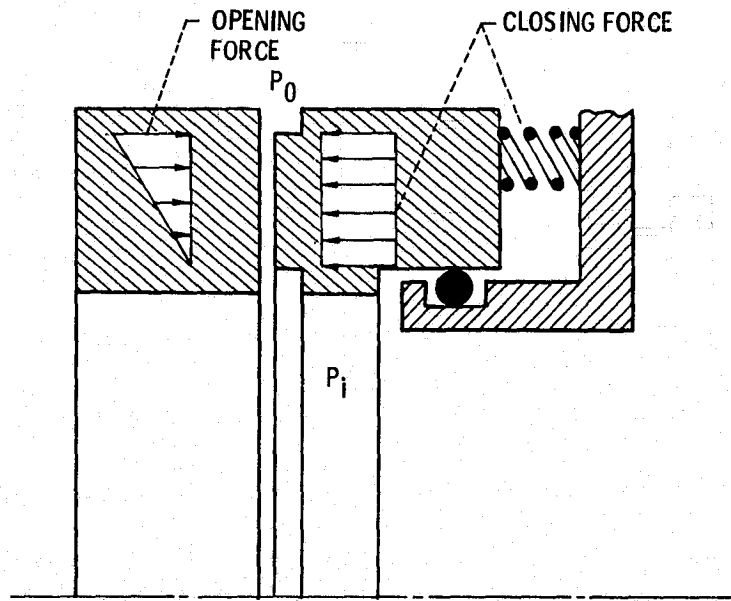
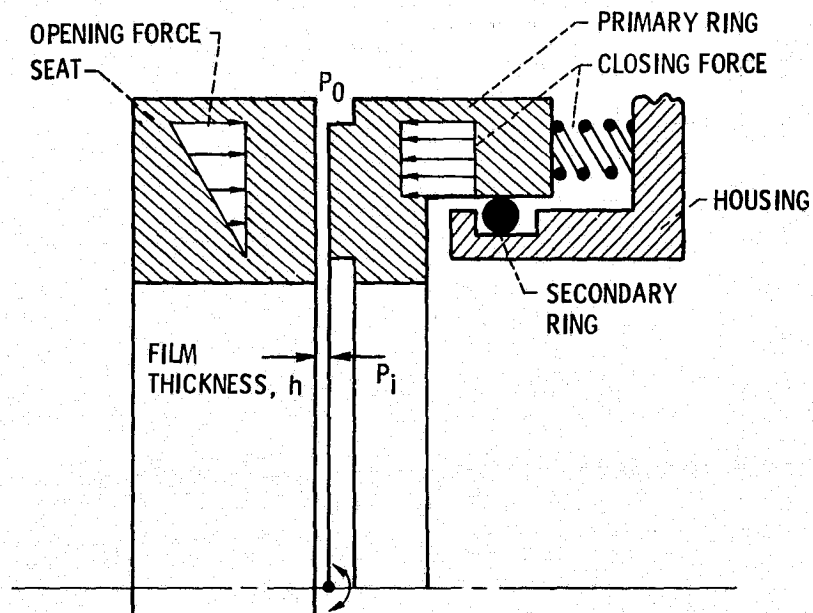


Figure 9. - Friction forces acting on secondary-seal ring.



(a) UNBALANCED SEAL ($P_0 > P_i$).



(b) BALANCED SEAL ($P_0 > P_i$).

Figure 10. - Seal opening and closing forces.

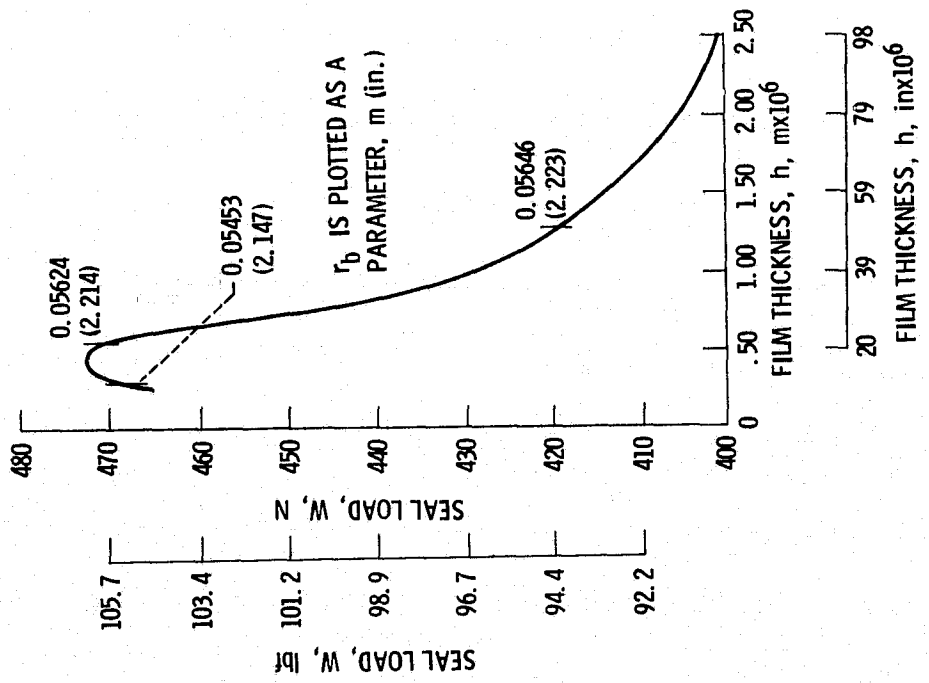
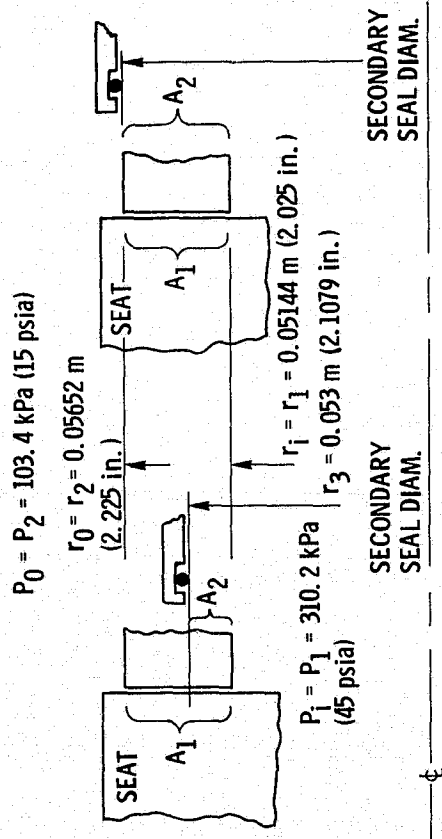


Figure 12. - Seal load at various film thicknesses for an inside seal. $P_1 = 45.0$ psia (310.2 kPa), $P_2 = 15.0$ psia (103.4 kPa), $r_1 = 2.025$ inches (0.05144 m), $r_2 = 2.225$ inches (0.05652 m), $T_{\infty} = 230^{\circ}$ F (383 K), $\omega = 5000$ rpm (524 rad/s), $k = 60.2$ Btu/hr-ft²-F (104 W/m²-K). (From ref. 14.)



- | | |
|--|---|
| a. BALANCED SEAL | a. UNBALANCED SEAL |
| $\frac{A_2}{A_1} = 0.4$ | $\frac{A_2}{A_1} = 1$ |
| b. HYDRAULIC CLOSING FORCE, 142 N (32.0 lbf) | b. HYDRAULIC CLOSING FORCE, 356 N (80.1 lbf) |
| SPRING FORCE, N (10.0 lbf) | SPRING FORCE, 44.5 N (10.0 lbf) |
| TOTAL CLOSING FORCE, 187 N (42.0) | TOTAL CLOSING FORCE, 400 N (90.1 lbf) |
| c. LIQUID FILM HYDROSTATIC FORCE, N (40.0 lbf) | c. LIQUID/VAPOR OPENING FORCE (SEE FIG. 12), 400 N (90.1 lbf) |

Figure 11. - Effect of pressure balance on seal operating mode.

E-7238-2

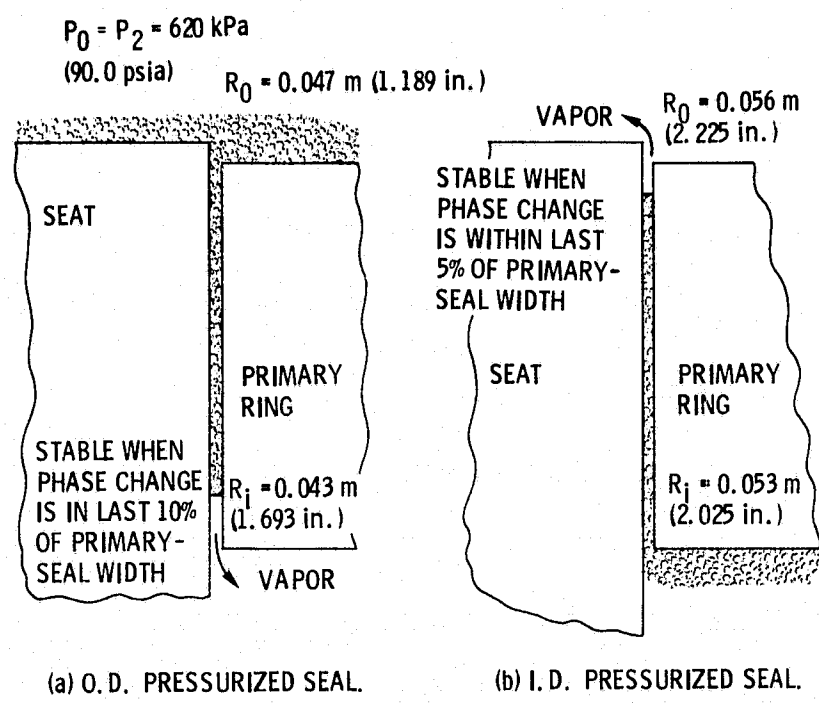


Figure 13. - Illustration of the location of the liquid/vapor interface for stable operation.